Optimum Equalization of Multicarrier Systems: A Unified Geometric Approach

Navid Lashkarian, *Member, IEEE,* and Sayfe Kiaei, *Senior Member, IEEE*

***Abstract*—This paper presents a new iterative equalization algorithm that maximizes capacity for discrete multitone (DMT) systems. The research modifies a previously proposed criterion and applies an appropriate transformation to map the objective function and the constraint set into a canonical region. The resulting constraint set exhibits an identifiable geometric characteristic. Using the gradient projection method in conjunction with projection onto convex sets (POCS) provides us with an iterative search algorithm that facilitates the gradient descent method. We also generalize the approach to two important subclasses of equalizers, namely linear phase and unit tap filters. We also derive a fundamental limit on the performance of the proposed approach. In comparison with the previous methods, the proposed equalization algorithm is less computationally complex and more geometrically intuitive. Simulation experiments confirm the validity of the proposed method for equalization of DMT systems.**

***Index Terms*—Capacity maximization, convex optimization, discrete multitone systems, multicarrier systems, optimum equalization, projection onto convex set.**

I. Introduction

DISCRETE multitone (DMT) systems provide an efficient method for partitioning the communication channel into a set of orthogonal subchannels. Prior to sending the data to the channel, a portion of transmit sequence, known as cyclic prefix (CP), is appended to the modulated symbol. The CP makes the channel-description matrix circulant, thus the orthogonal set of Fourier basis vectors can be applied to find its associated eigenvalues [16].

A short CP introduces less redundancy and thus improves the performance of data transmission. However, the length of the CP is lower bounded by the effective length of the channel [2]. In many practical channels, such as digital subscriber loops, the effective length of the channel is large, which results in a considerable performance loss due to adding the CP. The solution is to shorten the impulse response, through equalization, to a finite-impulse response (FIR) filter, known as the target impulse response (TIR), that is less disperse, which thus reduces the performance loss introduced by adding the CP [9]. In so doing, an FIR filter ($\mathbf{w}$), known as a time-domain equalizer (TEQ) is used at the receiving end.

Paper approved by G. M. Vitetta, the Editor for Equalization and Fading Channels of the IEEE Communications Society. Manuscript received September 12, 2000; revised January 2, 2001, and March, 22, 2001. This paper was presented in part at the IEEE International Conference on Communications (ICC), Vancouver, BC, Canada, June 1999.

N. Lashkarian is with Centillium Communications, Inc., Fremont, CA 94538 USA (e-mail: navid@centillium.com).

S. Kiaei is with the Department of Electrical Engineering, Arizona State University, Tempe, AZ 85287-5706 USA (e-mail: Sayfe@att.net).

Publisher Item Identifier S 0090-6778(01)09102-4.

In setting the coefficients of the TEQ, several criteria have been considered and investigated. Chow *et al.* provided an adaptive least mean square (LMS) algorithm for setting the coefficients of the TEQ [6]. Although it is simple in structure, the algorithm is not robust and globally optimum. Following this work, Al-Dhahir and Cioffi proposed a unified robust method that provides the optimum solution of the impulse response shortening problem based on minimum mean square error (MMSE) criterion [1]. Later, in a comprehensive study performed by the same authors, it was found that the solution obtained from MMSE approach may not necessarily optimize the performance (data rate) of the discrete multitone (DMT) system. Based on this observation, a new objective function was defined in which its solution approached theoretical performance level. Nevertheless, the proposed iterative solution, known as sequential quadratic programming (SQP), is a magnitude of order more complex with respect to the standard descent approach. This is mostly due to the fact that at each step of descent search in SQP, a quadratic constrained optimization subproblem [with complexity of $O(N^3)$] needs to be solved [13]. Furthermore, in each iteration of the descent search approach, a numerical approximate of the second-order Hessian matrix needs to be estimated. Due to this large overhead, the computational complexity of SQP far exceeds that of standard iterative descent methods.

This motivates our work in this paper. The research proposed in this paper takes advantage of the convex property of the constraint set to reformulate the original problem into a convex optimization problem. As a result, when combined with the projection onto convex set (POCS) technique, the stationary point obtained from the algorithm converges to an optimum point. POCS is a powerful technique which has found widespread applications in set theoretic signal processing algorithms and real-time applications [7].

The rest of this paper is organized as follows. Section II presents an overview of equalizer training approaches for DMT systems. In Section III, we present a new algorithm for training the DMT equalizer based on maximum data rate criterion. Section IV addresses the unit tap and linear phase constraints on the optimization problem and derives an upper bound on the performance of the algorithm. Finally, in Section V, the algorithm is applied to equalization of DMT systems.

II. Preliminaries

This section presents an overview of various TEQ methods for DMT systems as shown in Fig. 1. Throughout this paper, the symbols t, $*$, and $\tilde{.}$, represent transpose, Hermitian transpose, and Fourier transform operations, respectively. Matrices and

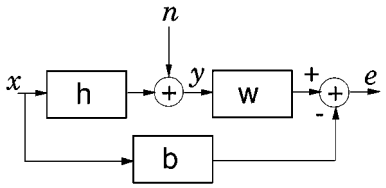

Fig. 1. Block diagram of the MMSE equalizer.

vectors are represented by upper-case and lower-case bold characters, respectively. The overall channel response is modeled as a discrete time FIR filter, expressed by $h = \{h_0, h_1, \ldots, h_v\}$ where v is the channel spread. The overall channel response includes the combined effect of the transmit and receive filters as well as the channel impulse response. Also, TEQ and TIR filters are assumed to be FIR filters with lengths N_f and N_b+1, respectively. The input signal x is an independent identically distributed random sequence with power of σ_x^2. As explained earlier, several objective functions can be used to optimize the performance of the TEQ. Among the existing methods, MMSE is known to be the most tractable technique for the impulse response shortening problem [1]. Several methods based on this approach have been proposed [10], [8]. In this approach, the optimum equalizer taps are computed to minimize the mean square error between output of the TIR and TEQ filters.

To avoid converging to the trivial solution, further constraint is imposed on the optimization problem. The unit energy constraint (UEC) requires the norm of TIR filter to be equal to one $(\mathbf{b}^*\mathbf{b} = 1)$, and the unit tap constraint (UTC) forces one of the taps in the TIR to be unity $(\mathbf{b}[k] = 1 | k \in \{0, 1, \ldots, N_b\})$.

Further investigations on optimizing the performance of DMT systems determined that the equalizer setting obtained by using the MMSE criterion would not necessarily result in the best geometrical signal-to-noise $(\mathrm{SNR}_{\mathrm{geom}})$ ratio. A new criterion for setting the coefficients of the TEQ equalizer to maximize the $\mathrm{SNR}_{\mathrm{geom}}$ was proposed in [3], [4]. According to this criterion, the optimum setting for TIR filter, which results in the maximum data rate criterion, is found by solving a dual constrained optimization problem as expressed by

$$\mathbf{b}_{\mathrm{opt}} = \arg\max_{\mathbf{b}} \sum_{i=1}^{N} \log_2 \mathbf{b}^* \mathbf{G}^{\mathbf{i}} \mathbf{b} \tag{1}$$

$$\text{s.t.} \quad \mathbf{C}_1\text{: } \mathbf{b}^*\mathbf{R}_{\boldsymbol{\Delta}}\mathbf{b} \leq \epsilon^{\mathbf{2}} \tag{2}$$

$$\mathbf{C}_2\text{: } \mathbf{b}^*\mathbf{b} = 1. \tag{3}$$

In (1), matrix $\mathbf{G}^i$ is defined as

$$\mathbf{G}^i \triangleq \mathbf{g}^i \mathbf{g}^{i^t}$$

where $\mathbf{g}^i$ is the ith Fourier basis vector given by

$$\mathbf{g}^i \triangleq [1 \quad e^{-j(2\pi i/N)} \quad \ldots \quad e^{-j(2\pi i N_b/N)}]^*.$$

The optimization problem given in (1) does not have a closed-form solution. In [3] and [4], the authors use standard optimization software tools in order to solve the above optimization problem. In the next section, we will present a new iterative gradient search algorithm for obtaining the optimum solution of the problem given in (1).

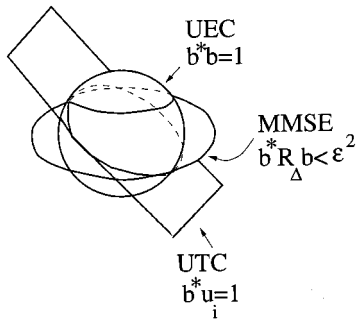

Fig. 2. Geometrical representation of the algorithm.

III. Proposed Iterative Gradient Search Algorithm

As explained in the previous section, the optimum equalization of DMT can be obtained by solving the constrained optimization problem given in (1). As depicted in Fig. 2, the constraint set for the problem given in (1) is the intersection of two regions. The first region $\mathbf{C}_1$: $\{\mathbf{b} \in R^{N_b+1} | \mathbf{b}^*\mathbf{R}_{\boldsymbol{\Delta}}\mathbf{b} \leq \epsilon^{\mathbf{2}}\}$ represents a closed set on the Euclidean space R^{N_b+1}. Geometrically, the set $\mathbf{C}_1$ represents an ellipsoid in R^{N_b+1}. Because of the symmetric property of the square matrix $\mathbf{R}_{\Delta}$, this constraint set exhibits a closed convex property on the Hilbert space. However, the unit energy constraint, $\mathbf{C}_2$: $\{\mathbf{b} \in R^{N_b+1} | \mathbf{b}^*\mathbf{b} = 1\}$, represents a region on the surface of a unit radial sphere that lacks convexity. In order to exploit the potential advantage of POCS, we remove the UEC from the constraint set. Unlike the MMSE approach, we can remove the UEC from the constraint set because origin is not among the local maximums of the objective function and no energy-boosting constraint is needed in order to avoid converging to the trivial solution. However, upon obtaining the global minimum, the solution vector can be normalized in order to satisfy the UEC. This scaling would not affect the geometrical signal-to-noise $(\mathrm{SNR}_{\mathrm{geom}})$ profile, as the TEQ coefficients would be scaled accordingly. Consequently, the mean square error and the additive noise contribution would be scaled by the same factor. Using the convexity property of the constraint set $\mathbf{C}_1$, along with a suitable iterative descent algorithm leads us to a stationary point. We considered the gradient projection method in order to find the feasible direction at each iteration.

Due to the symmetric property of the square matrix $\mathbf{R}_{\Delta}$, any N_b+1-dimensional vector $\mathbf{b}$ can be represented as a linear combination of N_b+1 orthogonal eigenvectors of matrix $\mathbf{R}_{\Delta}$ given by

$$\mathbf{b} = \alpha_0\mathbf{v}_0 + \alpha_1\mathbf{v}_1 + \cdots + \alpha_{N_b}\mathbf{v}_{N_b}, \quad \alpha_0, \alpha_1, \ldots, \alpha_{N_b} \in R \tag{4}$$

where $\mathbf{v}_m$ and λ_m are the mth normalized eigenvector and associated eigenvalue of matrix $\mathbf{R}_{\Delta}$ which satisfy

$$\mathbf{R}_{\Delta}\mathbf{v}_i = \lambda_i\mathbf{v}_i \quad \text{and} \quad \mathbf{v}_i^*\mathbf{v}_j = \delta[i-j]. \tag{5}$$

By substituting (4) into (1), the objective function can be expressed as

$$f = \sum_{i=1}^{N} \log_2 \left(\left(\sum_{j=0}^{N_b} \alpha_j \mathbf{v}_j \right)^* \mathbf{G^i} \left(\sum_{j=0}^{N_b} \alpha_j \mathbf{v}_j \right) \right)$$
$$= \sum_{i=1}^{N} \log_2 [\, \alpha_0 \quad \alpha_1 \quad \cdots \alpha_{N_b} \,] \mathbf{Q}^i [\, \alpha_0 \quad \alpha_1 \quad \cdots \alpha_{N_b} \,]^*$$

where the new matrix $\mathbf{Q}^i$ is defined as

$$\mathbf{Q}^i \triangleq \begin{bmatrix} \mathbf{v}_0^* \mathbf{G}^i \mathbf{v}_0 & \mathbf{v}_0^* \mathbf{G}^i \mathbf{v}_1 & \cdots & \mathbf{v}_0^* \mathbf{G}^i \mathbf{v}_{N_b} \\ \mathbf{v}_1^* \mathbf{G}^i \mathbf{v}_0 & \mathbf{v}_1^* \mathbf{G}^i \mathbf{v}_1 & \cdots & \mathbf{v}_1^* \mathbf{G}^i \mathbf{v}_{N_b} \\ \vdots & \vdots & \vdots & \vdots \\ \mathbf{v}_{N_b}^* \mathbf{G}^i \mathbf{v}_0 & \mathbf{v}_{N_b}^* \mathbf{G}^i \mathbf{v}_1 & \cdots & \mathbf{v}_{N_b}^* \mathbf{G}^i \mathbf{v}_{N_b} \end{bmatrix}.$$

Due to the properties of matrix $\mathbf{G}^i$, its (m, n)th entry can be computed efficiently as

$$\mathbf{Q}^i[m, n] = \tilde{\mathbf{v}}_m^*[i] \tilde{\mathbf{v}}_n[i]. \tag{6}$$

By virtue of (4), the constraint set $\mathbf{C}_1$ can be written as

$$\mathbf{b}^* \mathbf{R}_\Delta \mathbf{b} = \left(\sum_{j=0}^{N_b} \alpha_j \mathbf{v}_j \right)^* \mathbf{R}_\Delta \left(\sum_{j=0}^{N_b} \alpha_j \mathbf{v}_j \right)$$
$$= \lambda_0 \alpha_0^2 + \lambda_1 \alpha_1^2 + \cdots + \lambda_{N_b} \alpha_{N_b}^2 \le \epsilon^2.$$

Using this transformation, the optimization problem given in (1) subject to the constraint set $\mathbf{C}_1$ can be written as

$$\overline{\alpha}_{\text{opt}} = \arg\min_{\overline{\alpha}} \sum_{i=1}^{N} \log_2 \frac{1}{\overline{\alpha}^* \mathbf{Q}^i \overline{\alpha}}$$
$$\text{s.t.} \quad \mathbf{C}_1 \colon \alpha_0^2 \lambda_0 + \alpha_1^2 \lambda_1 + \cdots + \alpha_{N_b}^2 \lambda_{N_b} \le \epsilon^2$$

where $\overline{\alpha}$ is the projection vector given by

$$\overline{\boldsymbol{\alpha}} \triangleq [\, \alpha_0 \quad \alpha_1 \quad \cdots \quad \alpha_{N_b} \,]^*.$$

The principal drawback of the gradient projection method is the substantial overhead for computing the projection at each iteration. As we will address next, the canonical property of this constraint set enables us to perform the projection in an efficient way. The main idea with regard to the gradient projection method is that, in each iteration, a feasible direction is obtained by taking a step along a negative gradient followed by a projection onto the constraint set given by

$$\overline{\alpha}^{k+1} = \left[\overline{\alpha}^k - s^k \nabla f \left(\overline{\alpha}^k \right) \right]^+. \tag{7}$$

Here $[.]^+$ denotes the projection onto constraint set $\mathbf{C}_1$, s^k is a positive step-size, and ∇f is the gradient of the objective function given by

$$\nabla f = \frac{-1}{\ln 2} \sum_{i=1}^{N} \frac{(\mathbf{Q}^i + \mathbf{Q}^{i^t}) \overline{\alpha}}{\overline{\alpha}^* \mathbf{Q}^i \overline{\alpha}}. \tag{8}$$

There are several step size selection procedures for the gradient projection method. In order to simplify the search direction, we consider a constant step size $s^k = s$. As stated in [5, p. 215], the limit points of a sequence generated by the gradient projection with a constant step size are stationary, provided that s is limited in the range of $0 < s < 2/L$, wherein L is some constant satisfying

$$\|\nabla f(x) - \nabla f(y)\| \le L \|x - y\| \qquad \forall x, y \in X.$$

Next we derive the projection onto the convex set. Given a point $\overline{\alpha}^i \in R^{N_b+1}$, the projection of this point onto the set would be a point in the set such that it minimizes the distance $\|\overline{\alpha} - \overline{\beta}\|$ among all the points inside the set. In light of this fact, projection of a point $\overline{\alpha}_i \notin \mathbf{C}_1$ would be on the boundary of the set. Also, each point inside the constraint set would satisfy the constraint and would be projected onto itself. Therefore, the projection operator is defined as follows

$$[\boldsymbol{\alpha}]^+ = \begin{cases} \overline{\boldsymbol{\alpha}}, & \text{if } \overline{\boldsymbol{\alpha}} \in \mathbf{C}_1 \\ \overline{\boldsymbol{\beta}}, & \text{if } \overline{\boldsymbol{\alpha}} \notin \mathbf{C}_1 \end{cases}$$

where $\overline{\beta} = [\, \beta_0 \quad \beta_1 \quad \cdots \quad \beta_{N_b} \,]^*$ is a point in $\mathbf{C}_1$ which satisfies the constraint with equality

$$\mathbf{C}_1 = \left\{ \overline{\beta} \in R^{N_b+1} \,|\, \beta_0^2 \lambda_0 + \beta_1^2 \lambda_1 + \cdots + \beta_{N_b}^2 \lambda_{N_b} = \epsilon^2 \right\}.$$

To find this point, we construct the Lagrange functional

$$J(\overline{\boldsymbol{\beta}}, \gamma) = \left\| \overline{\boldsymbol{\beta}} - \overline{\boldsymbol{\alpha}} \right\|^2 + \gamma \left[\sum_{i=0}^{N_b} \lambda_i \beta_i^2 - \epsilon^2 \right]$$
$$= \sum_{i=0}^{N_b} \left[(\beta_i - \alpha_i)^2 + \gamma (\lambda_i \beta_i^2) \right] - \gamma \epsilon^2.$$

By taking the partial derivative of $J(\beta, \gamma)$ with respect to particular β_i, and setting it to zero, we obtain

$$\frac{\partial J(\overline{\boldsymbol{\beta}}, \gamma)}{\partial \beta_i} = 2(\beta_i - \alpha_i) + 2\gamma \lambda_i \beta_i$$
$$= 0$$
$$\beta_i = \frac{\alpha_i}{1 + \gamma \lambda_i}. \tag{9}$$

Also, taking the partial derivative of the Lagrangian functional with respect to Lagrange multiplier γ and setting it to zero provides the following:

$$\frac{\partial J(\overline{\boldsymbol{\beta}}, \gamma)}{\partial \gamma} = \sum_{i=0}^{N_b} (\beta_i)^2 \lambda_i - \epsilon^2 = 0. \tag{10}$$

Substituting (9) into the above equation provides

$$\psi(\gamma) \triangleq \frac{\partial J(\overline{\boldsymbol{\beta}}, \gamma)}{\partial \gamma} = \sum_{i=0}^{N_b} \left(\frac{\alpha_i}{1 + \gamma \lambda_i} \right)^2 \lambda_i - \epsilon^2 = 0. \tag{11}$$

Clearly (11) is a nonlinear equation in γ. It can be shown that, starting from $\gamma^0 = 0$, the iterates generated by Newton's method

$$\gamma^{k+1} = \gamma^k - \frac{\psi(\gamma^k)}{\psi'(\gamma^k)} \tag{12}$$

would always lead us to the unique positive solution of this equation. This results in a projection vector $\overline{\beta}$ that has a smaller

distance to $\overline{\alpha}$ than that furnished by use of any other root [14]. Upon computing the Lagrange multiplier γ from (12), the projection vector is found through (9).

A few additional remarks regarding the effect of initial condition are appropriate. First, the objective function lacks the convexity property. Therefore, the stationary point obtained from exploiting this algorithm is dependent upon the choice of initial condition. A proper choice of initial conditions leads us to a stationary point close to the optimal solution. A feasible initial condition can be the solution obtained from MMSE-UEC approach. As a second comment, in order for the algorithm to converge to a stationary point, the initial condition should be set so that the starting point satisfies the inequality constraint (feasible point). In the following sections, we investigate the effect of UTC and linear phase constraint on the optimization problem.

IV. Remarks

In some applications, it is desirable to impose a UTC on the TIR filter. This constraint forces the kth tap of the TIR filter to unity. Decision feedback equalization is a special case of UTC with $k = 0$. Including the UTC as a constraint equation in our optimization problem, the constraint set becomes the intersection of an ellipsoid and a hyperplane. The fundamental theorem of POCS defines a successive projection algorithm for solving the problem of finding a point in the intersection of several closed convex sets [14]. Based on this theorem, given two closed and convex sets C and D, the sequence X_n generated by the following algorithm:

$$X_{n+1} = P_D P_C X_n$$

where P_D and P_C denote, respectively, the projections onto D and C, will converge to a point $X^* \in H$, in the intersection of two sets. Given the vector $\overline{\alpha}$, projection of this vector over UTC, denoted as $\overline{\beta}$, can be obtained from (cf. Appendix - A)

$$\beta_i = \alpha_i - \frac{\sum_{j=0}^{N_b} \alpha_j \mathbf{v}_j[k] - 1}{\sum_{j=0}^{N_b} \mathbf{v}_j^2[k]} \mathbf{v}_i[k]. \tag{13}$$

In optimizing the performance of TEQ, the effect of phase distortion was not considered. In order to remove the phase distortion, linear phase constraint must be imposed on the TIR filter. This would add another constraint set to the previous problem increasing the complexity of the problem. The linear phase constraint is the intersection of hyperplanes in Euclidean space R^{N_b+1} that is both closed and convex. Therefore, projection onto convex sets can be extended to provide the optimum solution under linear phase constraint. Following, we provide the projection operator for linear phase type III filters [15]. The alternative constraints can be found in [12]. For linear phase type III filters, the projection operator is obtained (cf. Appendix - B) from

$$\beta_i = \alpha_i - \frac{1}{2} \sum_{k=0}^{(N_b/2)-1} \psi_k \tau_i[k] - \frac{1}{2} \psi_{(N_b/2)} \mathbf{v}_i \left[\frac{N_b}{2} \right], \quad i = 0, 1, \cdots, N_b \tag{14}$$

in which parameters $\tau_i[k]$ and ψ_k can be found from (18) and (22), respectively.

An upper-bound on objective function given in (1) can be obtained as follows:

$$\begin{aligned} \sum_{i=1}^{N} \log_2 \mathbf{b}^* \mathbf{G^i b} &= \log_2 \prod_{i=1}^{N} |\mathbf{b}^*.\mathbf{g^i}|^2 \\ &\overset{1}{\leq} log_{\mathbf{2}} \prod_{\mathbf{i=1}}^{\mathbf{N}} \|\mathbf{b}\|^2 \|\mathbf{g^i}\|^2 \\ &\overset{2}{\leq} \log_{\mathbf{2}} \left(\frac{\epsilon^{\mathbf{2}} (\mathbf{N_b} + \mathbf{1})^{\mathbf{2}}}{\lambda_{\min}(\mathbf{R_\Delta})} \right)^{\mathbf{N}}. \end{aligned}$$

Note that the first inequality follows from the Cauchy–Schwartz inequality while the second inequality is obtained from applying Rayleigh inequality as expressed by

$$\lambda_{\min}(\mathbf{R}_\Delta) \leq \frac{\mathbf{b}^* \mathbf{R_\Delta} \mathbf{b}}{\|\mathbf{b}\|^{\mathbf{2}}} \leq \lambda_{\max}(\mathbf{R}_\Delta)$$

where $\lambda_{\min}$ ($\lambda_{\max}$) is the minimum (maximum) eigenvalue of matrix $\mathbf{R}_\Delta$.

The above expression shows that increasing quadratic inequality constant (QIC) ϵ^2 would result in a larger upper-bound for the objective function. On the other hand, a smaller value for QIC causes the dual constraint problem given in (1) to better approximate the primary objective function [4]. This fact is consolidated through computer simulation in the subsequent section.

V. Simulations and Performance Evaluation of the Algorithms

In this section, we explore the potential performance achievable through the use of the proposed algorithm for equalization of DMT systems. We ran a series of simulations on CSA loops sampled at 276 kHz. The number of subchannels considered is $N = 64$. The TEQ and TIR are assumed to have lengths of $N_f = 17$ and $N_b = 4$, respectively. Receiver and thermal noise is modeled as additive white Gaussian noise (AWGN) with power of -30 dBm across the two-sided bandwidth. Near end cross-talk (NEXT) noise is modeled by exciting a coupling filter with spectrum of ($|H_x(f)|^2 = 10^{-13} f^{3/2}$) by a white Gaussian noise with power of 10 mW. Unless specified, signal power is set such that the matched filter bound (MFB $\triangleq \|h\|^2 \sigma_x^2 / \sigma_n^2$) of 15 dB is achieved at the receiving point. Furthermore, it is assumed that the power is uniformly distributed among the entire set of subchannels. In computing the data rate of the DMT system, the entire bandwidth is used and no limitation is imposed on the number of bits allocated for each subchannel. Also the noise margin and coding gain of 0 dB are assumed over the entire set of subchannels.

A. Effect of Channel-Impulse Response

In order to evaluate the performance of the proposed algorithm, computer simulations have been performed on a series of CSA loops. Fig. 3 shows the percentage of improvement in capacity with respect to the capacity obtained from MMSE–UEC approach. Decision delay, initial condition, and QIC are set to the settings furnished by the MMSE–UEC approach. Simulation results indicate that the algorithm exhibits robust

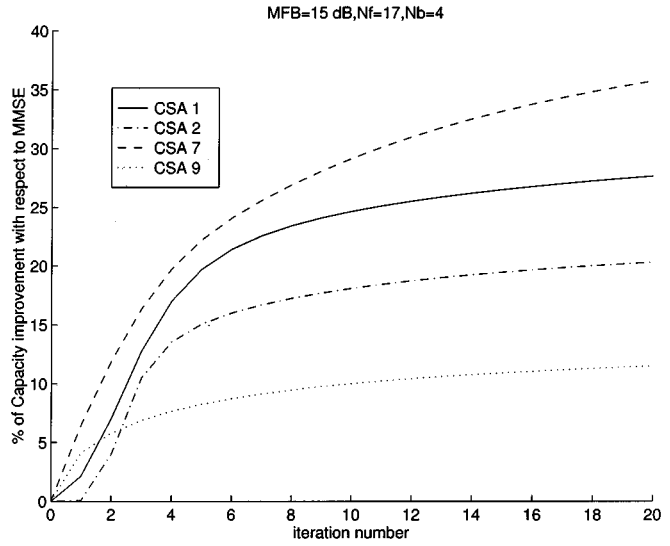

Fig. 3. Performance of the proposed algorithm for various CSA lines.

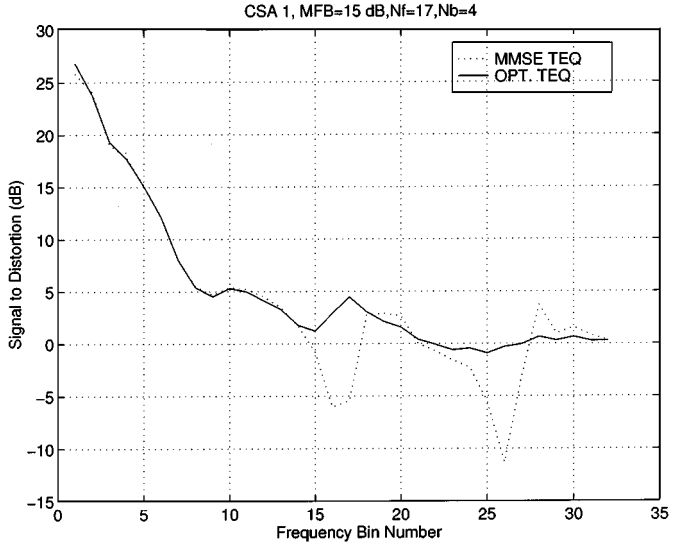

Fig. 4. Signal-to-distortion profile for MMSE-TEQ and max. Data rate TEQ.

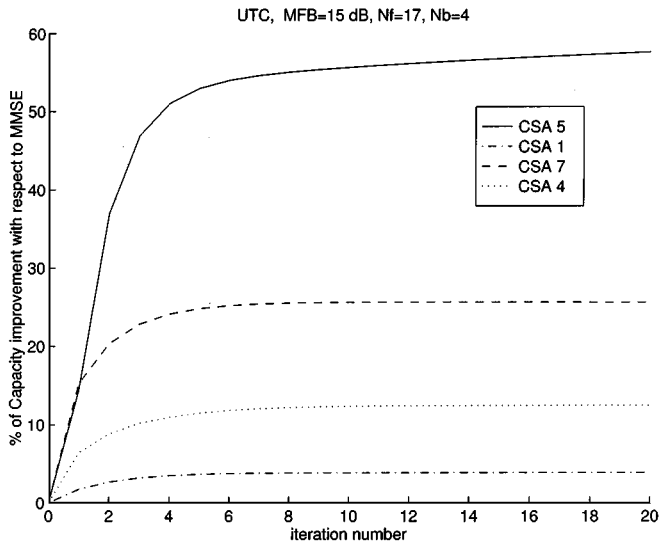

Fig. 5. Capacity profile versus decision delay and QIC.

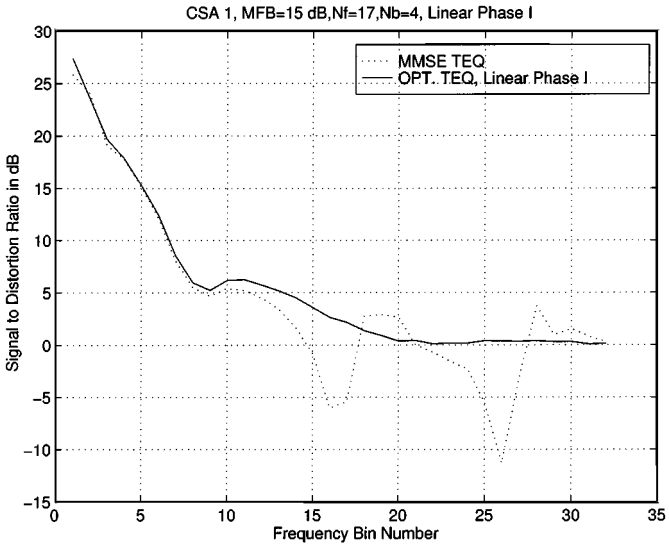

Fig. 6. Performance of the proposed algorithm under UTC.

convergence for all CSA loops used in the study. As shown in the figure, the capacity of the proposed method exceeds that of MMSE–UEC approach in the range of 10 to 35%. Fig. 4 compares the signal-to-distortion ratio of maximum capacity equalization against MMSE–UEC approach for the CSA-1 loop. As shown in the figure, the MMSE approach exhibits considerable performance degradation over half of the subchannels. This degradation can be viewed as sharp notches in the signal-to-distortion profile. Equalization of DMT based on maximum capacity outperforms the MMES–UEC approach by removing these nulls from the signal to distortion profile.

B. Effect of QIC (ϵ^2) and Decision Delay (Δ)

In order to investigate the effect of QIC, the proposed algorithm is applied for equalization of a typical CSA loop, namely CSA-6. Fig. 5 depicts the capacity profile as a joint function of QIC and decision delay. The QIC is set to $\epsilon^2 = K_e \epsilon^2_{\mathrm{MMSE}}$, where $K_e \in [0.2\ 1]$ and $\epsilon^2_{\mathrm{MMSE}}$ is the residual mean-square error obtained from the MMSE equalization. As stated previously, increasing QIC would increase the volume of the constraint region that provides more freedom in the search direction. On the other hand, the dual optimization problem would better approximate the capacity maximization problem if QIC is small. As the figure shows, the maximum capacity is displaced downward as K_e increases from 0.2 to 1.

C. UTC and Effect of Unit Tap Index

Next we examine the effect of UTC on the optimum equalization of a DMT system. Fig. 6 shows the relative improvement in data rate for maximum data rate equalization under UTC for various CSA lines. In optimizing the performance of the equalizer, QIC, decision delay, and unit tap index are set to the optimum values obtained from the MMSE-UTC approach. Changing the unit tap index of the TIR filter results in a different normal vector for the constraint hyperplane that shapes the constraint region

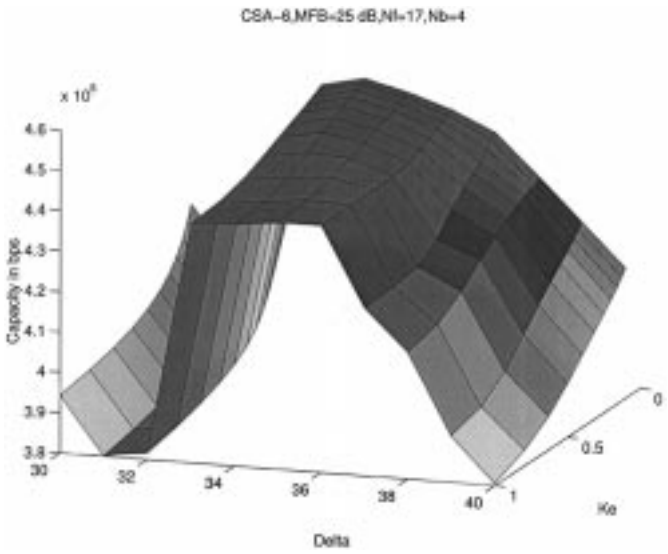

Fig. 7. Capacity profile versus decision delay and unit tap index.

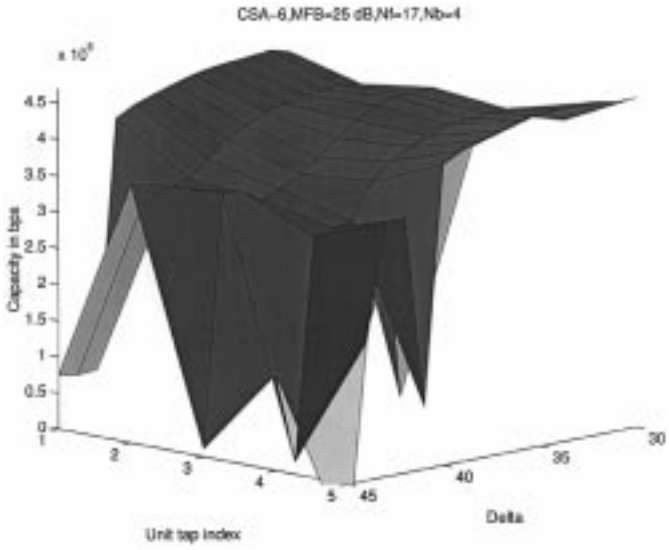

Fig. 8. Signal-to-distortion ratio for MMSE-TEQ and Max Capacity-TEQ with linear phase type (I) constraint.

accordingly. The optimum unit tap index k is found through performing exhaustive search on values k ranging from 1 to N_b+1. In order to show how the unit tap index of TIR can affect the performance of the proposed algorithm, the optimum equalization algorithm is performed on a typical CSA loop. Fig. 7 depicts the capacity profile as a joint function of decision delay and unit tap index k for CSA-1 loop. As the figure shows, a noncausal TIR would maximizes the performance of the DMT system for this particular case.

D. Effect of Phase Distortion

In order to investigate the effect of phase nonlinearity on the performance of DMT systems, we impose the linear phase constraint on the maximum capacity equalization problem. We consider the CSA-1 loop used in Section V-A and impose the linear phase type I constraint on the optimum equalization. Fig. 8 shows the signal-to-distortion ratio over subchannels

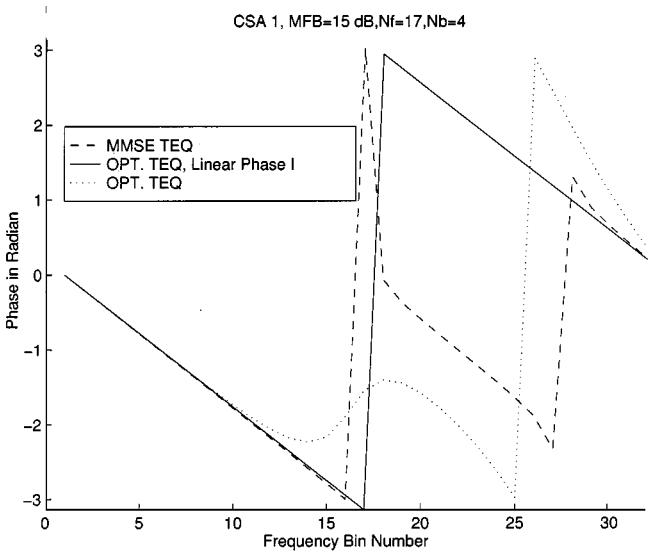

Fig. 9. Comparison between phase response of TIR filter under various constraints.

TABLE I
ALGORITHM SUMMARY AND CORRESPONDING COMPUTATIONAL COMPLEXITY

Operation	Flops
1. Initialization:	
1.1 Toeplitz Matrix Inversion (eq. 3)	$O(N_f^2)$
1.2 Hessian matrix Formation (eq. 3)	$N_f^2(N_b+1)+N_f(N_b+1)^2$
1.3 Eigenvalue Decomposition (eq. 5)	$O((N_b+1)^3)$
2. Iteration:	
2.1 Gradient Computation (eq. 8)	$O(\bar{N}(N_b+1)^2)$
2.2 Descent Update (eq. 7)	$O(N_b+1)$
2.3 Projection:	
2.3.1 Lagrange Computation (eq. 12)	$O(N_b+1)$
2.3.2 Elliposoid Projection (eq. 9)	$O(N_b+1)$

for this experiment. Fig. 9 compares the phase response of the TIR for MMSE-UEC, optimum capacity equalization, and optimum capacity equalization with linear phase constraint. As expected, the optimum capacity equalization with linear phase outperforms the other schemes through removing the phase distortion from the frequency response.

VI. CONCLUSION

Optimum equalization of multicarrier systems can be viewed as a constrained optimization problem over convex sets. The constraint sets exhibit identifiable geometrical characteristics which make the projection operation significantly efficient. Based on these observations, we have proposed a novel iterative algorithm as a straightforward application of POCS for solving the optimum equalization of multicarrier systems. Computational complexity of the algorithm is summarized in Table I.

APPENDIX

In this section, we obtain the projection operator for UTC and linear phase constraints.

A. Unit Tap Constraint

As we expressed earlier, the UTC forces the kth element of TIR filter to unity. Using (4), we can represent the kth element of TIR as a linear combination of the kth elements of orthogonal eigenvectors of matrix $\mathbf{R}_{\Delta}$. Consequently, the UTC set ($\mathbf{C}_3$) can be formulated as

$$\mathbf{C}_3 = \left\{ \overline{\beta} \in R^{N_b+1} \left| \sum_{j=0}^{N_b} \beta_j \mathbf{v}_j[k] = 1 \right. \right\}. \tag{15}$$

The above equation conforms a hyperplane in R^{N_b+1} which is both closed and convex. In general, the projection operator is a vector $\overline{\beta}$ which minimizes the Lagrange functional, i.e.,

$$J(\overline{\beta}, \psi) = \left\| \overline{\boldsymbol{\beta}} - \overline{\boldsymbol{\alpha}} \right\|^2 + \psi \left(\sum_{j=0}^{N_b} \beta_j \mathbf{v}_j[k] - 1 \right). \tag{16}$$

As shown in [11], the projection operator for this constraint is obtained as follows:

$$\begin{aligned} \beta_i &= \alpha_i - \frac{\psi}{2} \mathbf{v}_i[k] \\ \psi &= 2 \frac{\sum_{j=0}^{N_b} \alpha_j \mathbf{v}_j[k] - 1}{\sum_{j=0}^{N_b} \mathbf{v}_j^2[k]}. \end{aligned} \tag{17}$$

The above equation along with (17) results in the projection operator as given in (13).

B. Linear Phase Type III

Linear phase type III filters satisfy the antisymmetry property as expressed by

$$\mathbf{b}[n] = \begin{cases} -\mathbf{b}[N_b - n] & n = 0, \ldots, \dfrac{N_b}{2} - 1 \\ 0 & \dfrac{N_b}{2}. \end{cases}$$

The first constraint is the intersection of hyperplanes in R^{N_b+1}. Using the orthogonal eigen-vectors of the Hessian matrix $\mathbf{R}_{\Delta}$, this constraint set can be expressed as

$$\sum_{j=0}^{N_b} \beta_j \mathbf{v}_j[k] = \sum_{j=0}^{N_b} \beta_j \mathbf{v}_j[N_b - k], \qquad k = 0, 1, \ldots, \frac{N_b}{2} - 1$$

which conforms to the following constraint set:

$$\mathbf{C}_4 = \left\{ \overline{\beta} \in R^{N_b+1} \left| \sum_{j=0}^{N_b} \beta_j \rho_j[k] = 0 \right. \right. \qquad \left. \left. k = 0, 1, \ldots, \frac{N_b}{2} - 1 \right\}.$$

Similarly, the second constraint can be viewed as another hyperplane in R^{N_b+1} which encounters origin and can be represented as

$$\mathbf{b}\left[\frac{N_b}{2}\right] = \sum_{j=0}^{N_b} \beta_j \mathbf{v}_j \left[\frac{N_b}{2}\right] = 0.$$

Using the above equations, the Lagrangian functional can be written as

$$J\left(\overline{\boldsymbol{\beta}}, \overline{\psi}\right) = \left\| \overline{\beta} - \overline{\boldsymbol{\alpha}} \right\|^2 + \sum_{k=0}^{(N_b/2)-1} \psi_k \sum_{j=0}^{N_b} \beta_j \tau_j[k] + \psi_{N_b/2} \sum_{j=0}^{N_b} \beta_j \mathbf{v}_j \left[\frac{N_b}{2}\right]$$

where the variables $\tau_j[n]$ and $\overline{\psi}$ are defined as

$$\tau_j[n] \triangleq \mathbf{v}_j[n] + \mathbf{v}_j[N_b - n] \tag{18}$$

$$\overline{\psi} \triangleq \begin{bmatrix} \psi_0 & \psi_1 & \cdots & \psi_{N_b/2} \end{bmatrix}^*. \tag{19}$$

It can be shown [12] that the projector operator for this constraint is in the following form:

$$\beta_i = \alpha_i - \frac{1}{2} \sum_{k=0}^{(N_b/2)-1} \psi_k \tau_i[k] - \frac{1}{2} \psi_{N_b/2} \mathbf{v}_i \left[\frac{N_b}{2}\right] \tag{20}$$

where the Lagrange functionals are the solution to the following set of linear equations:

$$\boldsymbol{\Gamma} \boldsymbol{\psi} = \mathbf{r} \tag{21}$$

where the matrix $\boldsymbol{\Gamma}$ and vector $\mathbf{r}$ are defined as

$$\boldsymbol{\Gamma}[m, n] \triangleq \begin{cases} \sum_{j=0}^{N_b} \tau_j[m] \tau_j[n], & m, n = 0, \ldots, \frac{N_b}{2} - 1 \\ \sum_{j=0}^{N_b} \tau_j[n] \mathbf{v}_j \left[\frac{N_b}{2}\right], & m = \frac{N_b}{2} \,\&\, n = 0, \ldots, \frac{N_b}{2} - 1 \\ \sum_{j=0}^{N_b} \tau_j[m] \mathbf{v}_j \left[\frac{N_b}{2}\right], & n = \frac{N_b}{2} \,\&\, m = 0, \ldots, \frac{N_b}{2} - 1 \\ \sum_{j=0}^{N_b} \mathbf{v}_j \left[\frac{N_b}{2}\right]^2, & m = n = \frac{N_b}{2} \end{cases}$$

$$\mathbf{r}[n] \triangleq \begin{cases} 2 \sum_{j=0}^{N_b} \tau_j[m] \alpha_j, & n = 0, 1, \ldots, \frac{N_b}{2} - 1 \\ 2 \sum_{j=0}^{N_b} \alpha_j \mathbf{v}_j \left[\frac{N_b}{2}\right], & n = \frac{N_b}{2}. \end{cases}$$

The Lagrangian multiplier vector can be obtained through successive iteration of POCS algorithm or simply through inverting the matrix Γ as follows:

$$\boldsymbol{\psi} = \boldsymbol{\Gamma}^{-1} \mathbf{r}. \tag{22}$$

ACKNOWLEDGMENT

The authors thank the anonymous reviewers for constructive comments that helped to clarify technical points and improve the presentation.

REFERENCES

[1] N. Al-Dhahir and J. Cioffi, "Efficiently computed reduced-parameter input-aided MMSE equalizers for ML detection: A unified approach," *IEEE Trans. Inform. Theory*, vol. IT-42, pp. 903–915, May 1996.

[2] A. Peled and A. Ruiz, "Frequency domain data transmission using reduced computational complexity algorithms," in *IEEE Int. Conf. on Acoustics, Speech and Signal Processing*, Denver, CO, Apr. 1980, pp. 964–967.

[3] N. Al-Dhahir and J. Cioffi, "A bandwidth-optimized reduced-complexity equalized multicarrier transceiver," *IEEE Trans. Commun.*, vol. 45, pp. 948–956, May 1997.

[4] ——, "Optimum finite-length equalization for multicarrier transceivers," *IEEE Trans. Commun.*, vol. 44, pp. 56–63, Jan. 1996.

[5] D. P. Berstekas, *Nonlinear Programming*. Belmont, MA: Athena Scientific, 1995.

[6] J. Chow, J. Cioffi, and J. A. Bingham, "Equalizer training algorithms for the multicarrier modulation systems," in *Int. Conf. Communication*, Geneva, Switzerland, May 1993, pp. 948–952.

[7] P. Combettes, "The foundation of set theoretic estimation," *Proc. IEEE*, vol. 81, pp. 182–208, Feb. 1993.

[8] I. Lee, J. S. Chow, and J. Cioffi, "Performance evaluation of a fast computation algorithm for the DMT in high-speed subscriber loop," *IEEE J. Select. Areas Commun.*, vol. 13, pp. 1564–1570, Dec. 1995.

[9] J. S. Chow and J. M. Cioffi, "A cost-effective maximum likelihood receiver for multicarrier systems," in *IEEE Int. Conf. Communications*, vol. 2, June 1992, pp. 948–952.

[10] N. Lashkarian and S. Kiaei, "Fast algorithm for finite-length MMSE equalizers with application to discrete multitone systems," in *IEEE Int. Conf. on Acoustics, Speech, and Signal Processing*, vol. 5, Phoenix, AZ, Mar. 1999, pp. 2753–2756.

[11] N. Lashkarian and S. Kiaei, "Optimum equalization of multi-carrier systems via projection onto convex set," in *IEEE Int. Conf. on Communications*, vol. 2, Vancouver, BC, Canada, June 1999, pp. 968–972.

[12] N. Lashkarian, " Optimum equalization and synchronization of broadband multicarrier systems," Ph.D. dissertation, Oregon State University, Corvallis, June 1999.

[13] N. Al-Dhahir, "Throughput-maximizing FIR transmit filters for linear disperse channels," *IEEE Trans. Commun.*, vol. 46, pp. 1438–1442, Nov. 1998.

[14] H. Stark and Y. Yang, *Vector Space Projection*. New York: Wiley, 1998.

[15] A. Oppenheim and R. Schafer, *Discrete-Time Signal Processing*. Englewood Cliffs, NJ: Prentice-Hall, 1989.

[16] J. Cioffi, "Course Notes for ECE379 C'," Stanford University, Stanford, CA.

Navid Lashkarian (S'98–A'99) received the B.Sc. and M.S. degrees (with highest honors) from Tehran University, Tehran, Iran, and the Ph.D. degree from Oregon State University, Corvallis, all in electrical engineering, in 1990, 1992, and 1999, respectively.

During 1992 to 1995, he was a full-time faculty Lecturer at the Department of Electrical and Computer Engineering at Tehran University. From 1995 to 1999, he was a Research Assistant at the Electrical and Computer Engineering Department at Oregon State University where he conducted research on broad-band multi-carrier communications. He is currently a Senior Research and Development Engineer at Centillium Communications, Inc., Fremont, CA, where he is involved in the design and development of high-speed broad-band xDSL modems. His research interest focuses primarily on digital communications, statistical signal processing, wavelet and multi-resolution analysis, and DSP and VLSI applications.

Sayfe Kiaei (S'86–M'87–SM'93) received the Ph.D. degree from Washington State University in 1987.

He has been with Arizona State University since January 2001. He is currently a Professor in the Electrical Engineering Department and the Director of Communications and Mixed-Signals Research Center. He was with Motorola Inc. from 1993 to 2001 as a Senior Member of Technical Staff with the Wireless Technology Center at Motorola responsible for the development of Wireless Transceiver ICs. Prior to that, he was with the Braodband Products Operations responsible for research and development of xDSL systems design. He was an Associate Professor at Oregon State University, Corvallis, before joining Motorola where he had taught CMOS IC design and wireless systems. His research area is in telecommunications, VLSI and DSP development. He assisted in the establishment of the Industry–University Center for the Design of Analog/Digital ICs (CDADIC) and served as a Co-Director of CDADIC for 10 years. CDADIC is a research center for mixed-signal IC design representing four universities (Oregon State University, Washington State University, University of Washington, and State University of New York), over 25 high-tech electronics companies, and National Science Foundations. Prior to this, he was employed at Boeing's Flight Systems Research and Technology Center as Hardware Design Engineer and CAD tool development for airplane controllers. He has published over 50 journal and conference papers and patents.

Dr. Sayfe has received four major research awards and was presented the Carter Best Teacher Award by students and faculty of Oregon State College of Engineering. He is the recipient of the IEEE's Darlington Award for the best paper in the IEEE TRANSACTIONS ON CIRCUITS AND SYSTEMS for a paper on low-noise circuits for mixed-signal ICs. He has served in various editorial capacities for the IEEE Communications Society. He has been active in numerous conference events as conference chairman, technical program chair, or member of technical program committees.